Investigation of the Long Term Effects of Magnesium Chloride and Other Concentrated Salt Solutions on Pavement and Structural Portland Cement Concrete

Project Number: SD2002-01

Submitted by:

Lawrence L. Sutter, Ph.D.
Michigan Tech
1400 Townsend Dr.
Houghton, MI 49931

Quarterly Report

Overview

This Quarterly Report is submitted to outline the work accomplished during the reporting period 7-15-05 to 10-15-05, identify problems (current and anticipated), and to describe any deviations from the agreed Work Plan. This Quarterly Report is arranged by the Tasks described in the project Work Plan. The following is a summary of results for this reporting period.

- Preliminary petrographic analysis of field cores obtained from selected bridge decks in Montana has been conducted.
- Phase II ASTM C 672 testing of concrete mixes has been suspended.
- A new approach to Phase II is proposed.

Task Report

Task 1: Literature Review

Task 1 Completion - 100%

Task 2: Conduct Survey

Task 2 Completion - 100%

Task 3: Site Selection

Task 3 Completion -100%

Task 4: Meeting with Technical Panel

Task 4 Completion -100%

Task 5: Characterization of Field Specimens

Work under Task 5 has this reporting period focused on analysis of cores obtained from selected bridge decks in Montana. The preliminary results of this investigation are provided below.

Petrographic Examination of Cores from Bridge Decks West of Missoula, Montana

Field Observations
Cores were taken from two bridge decks on Interstate 90 west of Missoula, Montana. Two cores were taken from each bridge deck, one adjacent to visible deterioration, and another away from the deterioration.

Figure 1 shows the first site, the eastbound bridge deck of the Tarkio interchange. Both core holes are visible in Figure 1, along with several areas covered with cold-patch material. The core taken adjacent to the deterioration (core T-1) did not penetrate the entire bridge deck. The core taken away from the deterioration (core T-2) did penetrate the deck, as is shown in Figure 2, a photo taken from beneath the bridge deck. Although core T-1 did not penetrate the deck, water seeping through cracks from the coring operation is visible in Figure 2. Also visible in Figure 2 are areas of white efflorescence situated directly below the deteriorated portions from the surface of the bridge deck. Figures 3 and 4 show core T-1, with a large crack plane oriented parallel to the pavement surface at a depth of approximately 4 cm. Figure 5 shows core T-2. No reinforcing steel was encountered in cores T-1 or T-2.

Figure 6 shows the second site, the westbound bridge deck of the Sloway interchange, after coring. Spalling of the pavement surface can be seen in Figure 6. Both cores penetrated the entire bridge deck. Also shown in the foreground of Figure 6 are markings

from a third aborted core attempt. Figure 7 shows a photo taken from beneath the bridge deck. The hole from the core taken adjacent to the deterioration, (core S-1) is clearly shown in the middle of Figure 7. The hole from the core taken away from the deterioration, (core S-2) is partly obscured by the pre-stressed beam, as seen in Figure 7. Figures 8 and 9 show core S-1, with a large rust-stained crack plane oriented parallel to the pavement surface at a depth of approximately 3 cm, just above the reinforcing steel. Figure 10 shows core S-2. Reinforcing steel was encountered in both cores S-1 and S-2.

Sample Preparation

Cores T-1 and S-1 were first embedded in fluorescent dyed epoxy resin, and then cut into slabs. The slabs were further cut into billets and prepared in thin section for examination with a petrographic microscope and a scanning electron microscope (SEM). Cores T-2 and S-2 were not embedded with epoxy, but also cut into slabs. From each of the non-embedded cores, one of the slabs was polished for examination with a desktop scanner and stereo microscope, and the other slab was cut into billets and prepared for chloride profiling with the x-ray microscope.

Desktop Scanner and Stereo-Microscope Observations

Figures 11 and 12 show scanned images of cores T-2 and S-2. The reinforcing steel of core S-2 is clearly visible in Figure 12. Figure 13 shows a close-up stereo microscope image of rust and cracks from the upper tier of steel reinforcement. Air-void analyses and chemical staining have not yet been performed on the polished slabs from cores T-2 and S-2.

Petrographic Microscope and SEM Observations

Figures 14 through 19 show elemental maps made from polished thin sections from core T-1. Figures 14, 15, and 16 represent a cross-section at the pavement surface. Figures 17, 18, and 19 represent a cross-section through the large crack at 4 cm depth. The magnesium maps of Figures 15 and 16 show pronounced magnesium enrichment of the hardened cement paste at the pavement surface. Magnesium enrichment is not evident at the crack at depth, as shown in Figures 18 and 19. The chlorine maps shown in Figures 14 and 16, and in Figures 17 and 19, do not show much chlorine enrichment. It should be noted, however, that the fluorescent dyed epoxy used to stabilize the samples also contains chlorine which can mask the residual chlorine that may be present from the deicer.

Figures 20 through 25 show elemental maps made from polished thin sections from core S-1. Figures 20, 21, and 22 represent a cross-section at the pavement surface. Figures 23, 24, and 25 represent a cross section through the large crack at 3 cm depth. Unlike the thin section prepared from core T-1, the thin section prepared to represent the cross-section at the pavement surface in core S-1 does not show pronounced magnesium enrichment, as shown in Figures 21 and 22. Magnesium enrichment is also not evident at the crack at depth, as shown in Figures 24 and 25. However, there is a chlorine enriched zone just above the crack at depth, as shown in Figures 23 and 25.

Figures 26a, 26b, 27a, and 27b show petrographic microscope images of the regions mapped on thin sections prepared from core S-1.

The thin sections prepared to represent a cross-section of the large crack at depth for both cores T-1 and S-1 exhibited pronounced depletion of calcium hydroxide in the hardened cement paste in a region of about 1 mm on either side of the crack. Petrographic work on these samples will continue to further investigate the alteration of the hardened cement paste within the vicinity of the large crack.

Chloride Profiling with X-ray Microscope

An x-ray microscope was used to collect characteristic Cl Kα x-rays from points at varying depths in the cement paste from billets prepared from cores T-2 and S-2. Figures 28 and 29 show profiles obtained from core T-2, whereas Figures 30 and 31 show profiles obtained from core S-2. As shown in Figures 28 and 29, chloride concentrations drop to negligible levels at a depth between 70 and 90 mm for the samples prepared from core S-2. As shown in Figures 30 and 31, chloride concentrations are still in the range of 0.25 to 0.50 percent at depths of 70 to 90 mm for the samples prepared from core T-2. Additional points at depths greater than 90 mm have yet to be collected from samples prepared from core T-2.

Conclusions

The deterioration at both sites is characterized by a crack plane oriented parallel to the pavement surface at a depth between 3 and 4 cm. In the case of the Sloway bridge deck, the depth of this crack plane coincides with the position of the reinforcing steel. Rust was observed associated with the reinforcing steel encountered at these depths. No reinforcing steel was encountered in cores from the Tarkio bridge deck. The thin sections prepared from the Tarkio bridge deck showed magnesium enrichment at the pavement surface similar to the magnesium enrichment observed in the constant cold temperature $MgCl_2$ brine mortar cylinder experiment. Magnesium enrichment was not evident in thin sections prepared from the Sloway bridge deck. Both bridge decks exhibited calcium hydroxide depletion of the cement paste in the immediate vicinity of the large crack at depth. Calcium hydroxide depletion was also pronounced in the cracked portions of the mortar cylinders from the constant cold $MgCl_2$ brine experiment. However, unlike the brine experiment, no calcium oxychloride phases were observed in any of the cracks from the bridge decks. The pronounced chlorine concentration above the large crack at 3 cm depth as shown in the elemental maps from the polished thin section prepared from the Sloway bridge deck shows that chloride rich fluids were present in the crack.

Task 5 Problems and/or Deviations from Work Plan

There were no problems or deviations for Task 5 incurred during the reporting period.

Task 5 Completion -55%

Figure 1: EB I-90 Tarkio interchange bridge deck after coring.

Figure 2: Beneath EB I-90 Tarkio interchange after coring.

Figure 3: Core T-1, taken adjacent to deteriorated area.

Figure 4: Core T-1, separated to illustrate crack plane.

Figure 5: Core T-2, taken away from deteriorated area.

Figure 6: WB I-90 Sloway interchange bridge deck after coring.

Figure 7: Beneath WB I-90 Sloway interchange after coring.

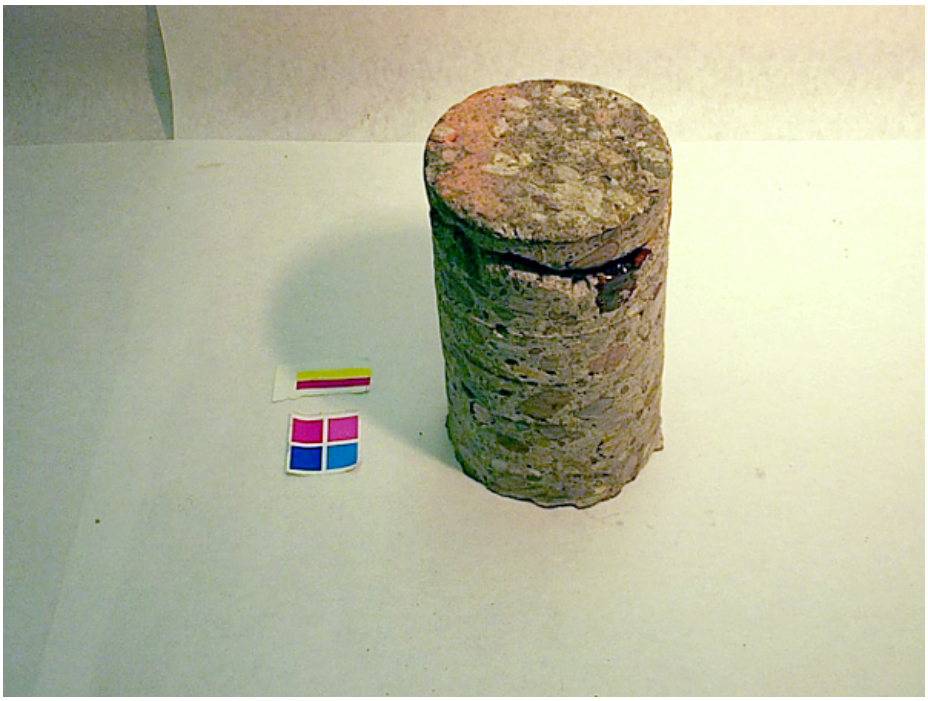

Figure 8: Core S-1, taken adjacent to deteriorated area.

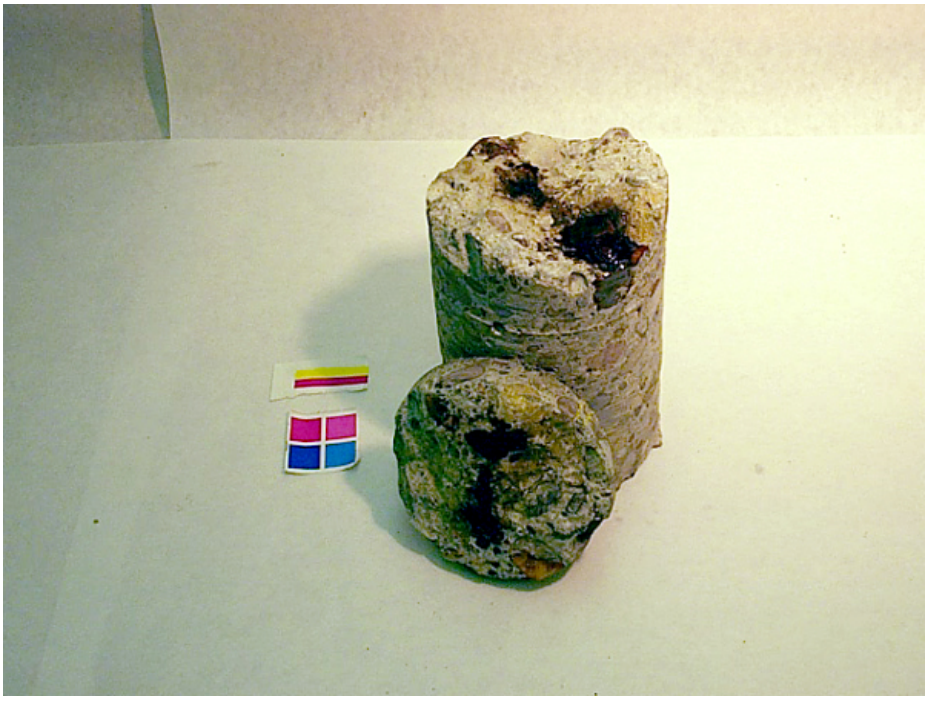

Figure 9: Core S-1, separated to illustrate crack plane.

Figure 10: Core S-2, taken away from deteriorated area.

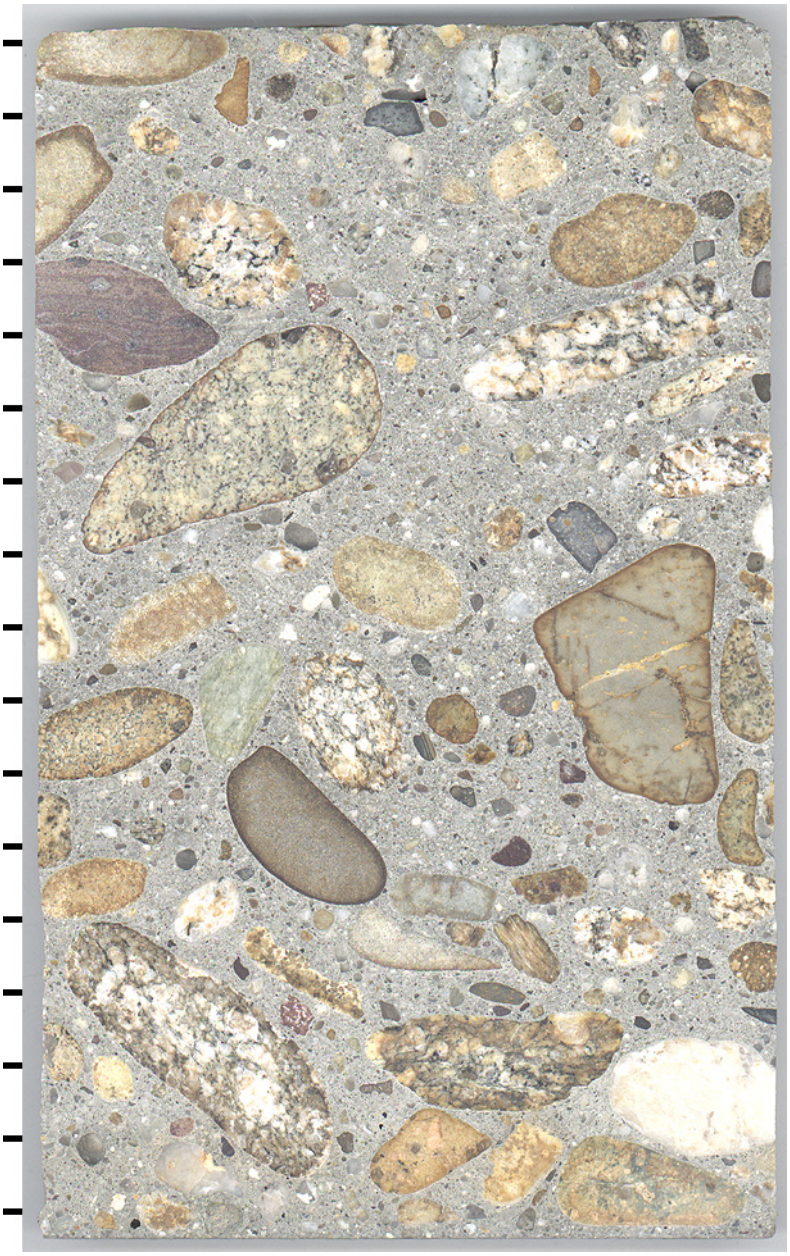

Figure 11: Polished slab from core T-2, tic marks every cm.

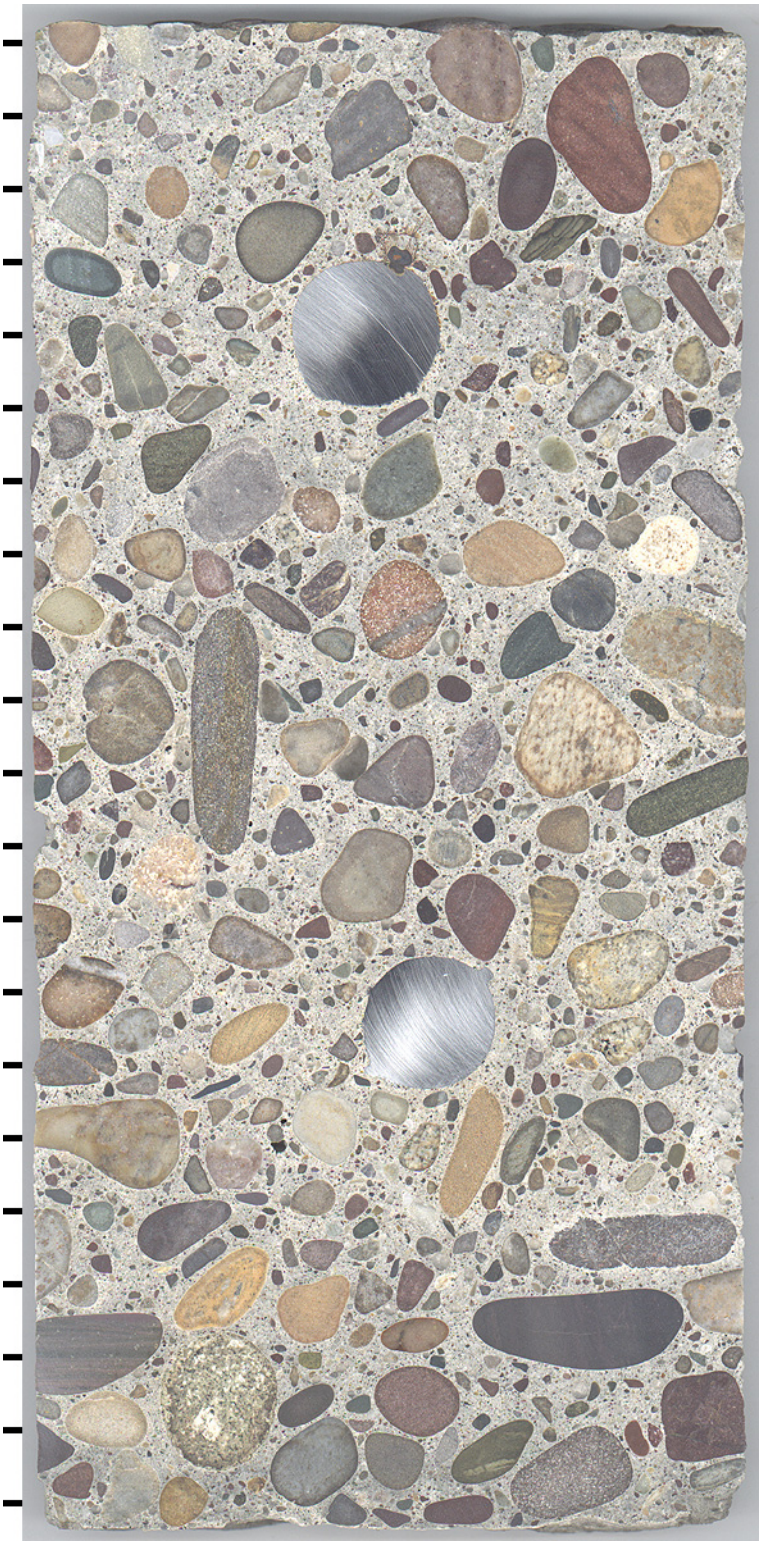

Figure 12: Polished slab from core S-2, tic marks every cm.

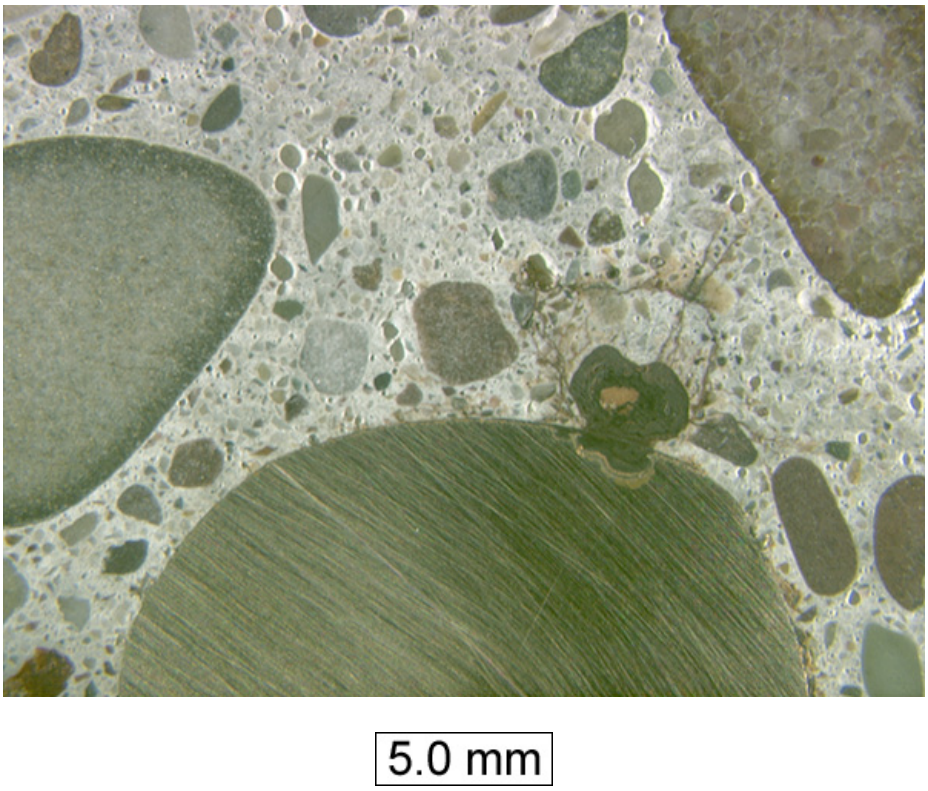

Figure 13: Stereo microscope image of rust along top of reinforcing steel as exposed on polished slab from core S-2.

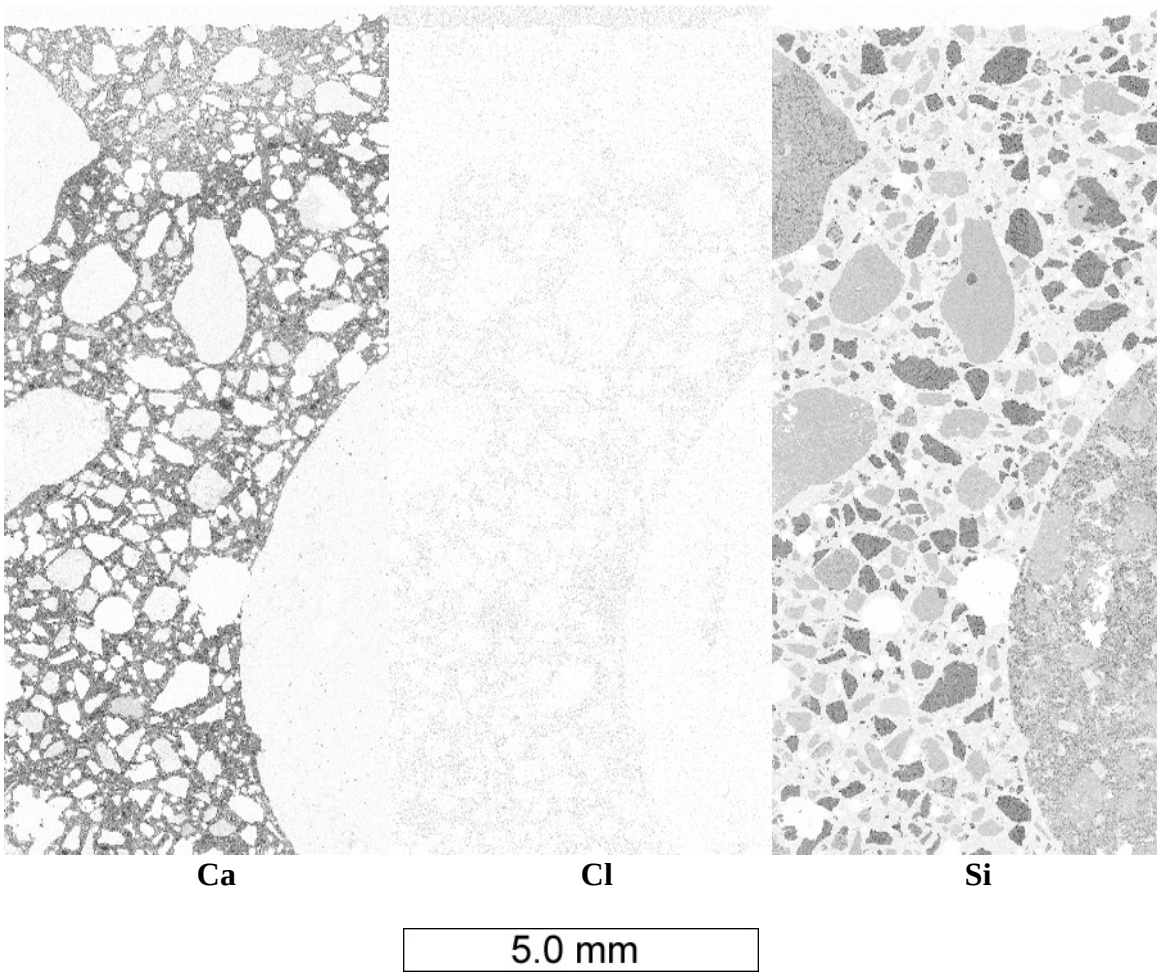

Figure 14: Characteristic Kα x-ray maps showing concentrations for calcium, chlorine, and silicon from polished thin section prepared from core T-1 showing cross section through pavement surface. Darker regions correspond to higher x-ray counts.

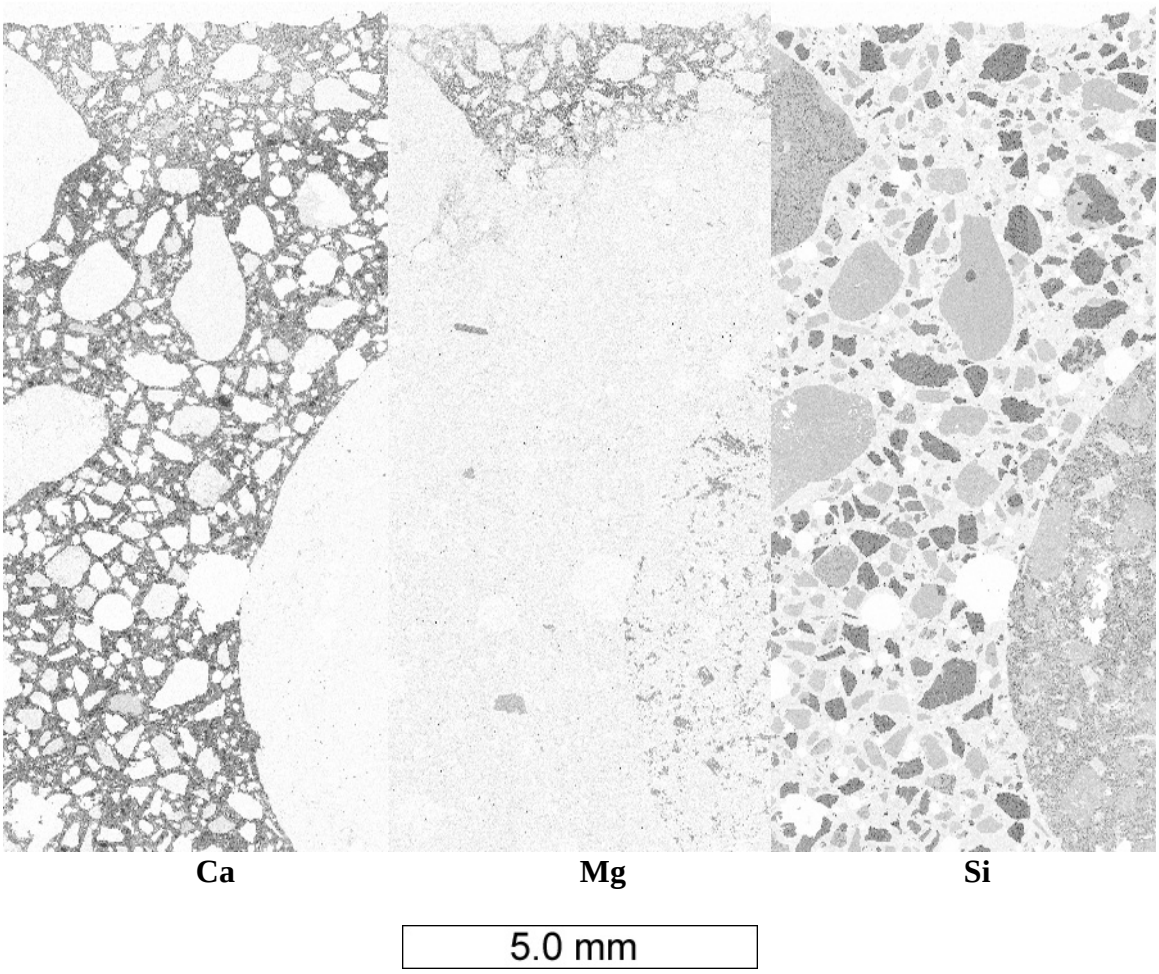

Figure 14: Characteristic Kα x-ray maps showing concentrations for calcium, magnesium, and silicon from polished thin section prepared from core T-1 showing cross section through pavement surface. Darker regions correspond to higher x-ray counts.

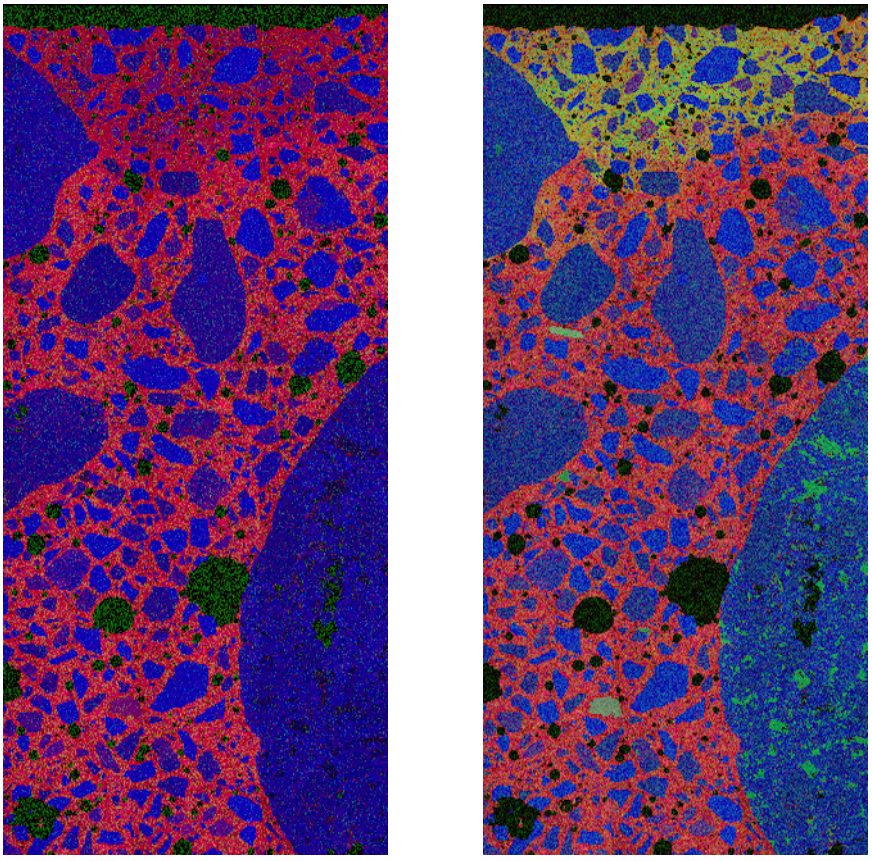

Figure 16: RGB composite image of characteristic Kα x-ray maps from polished thin section prepared from core T-1 showing cross section through pavement surface. Brighter regions correspond to higher x-ray counts.

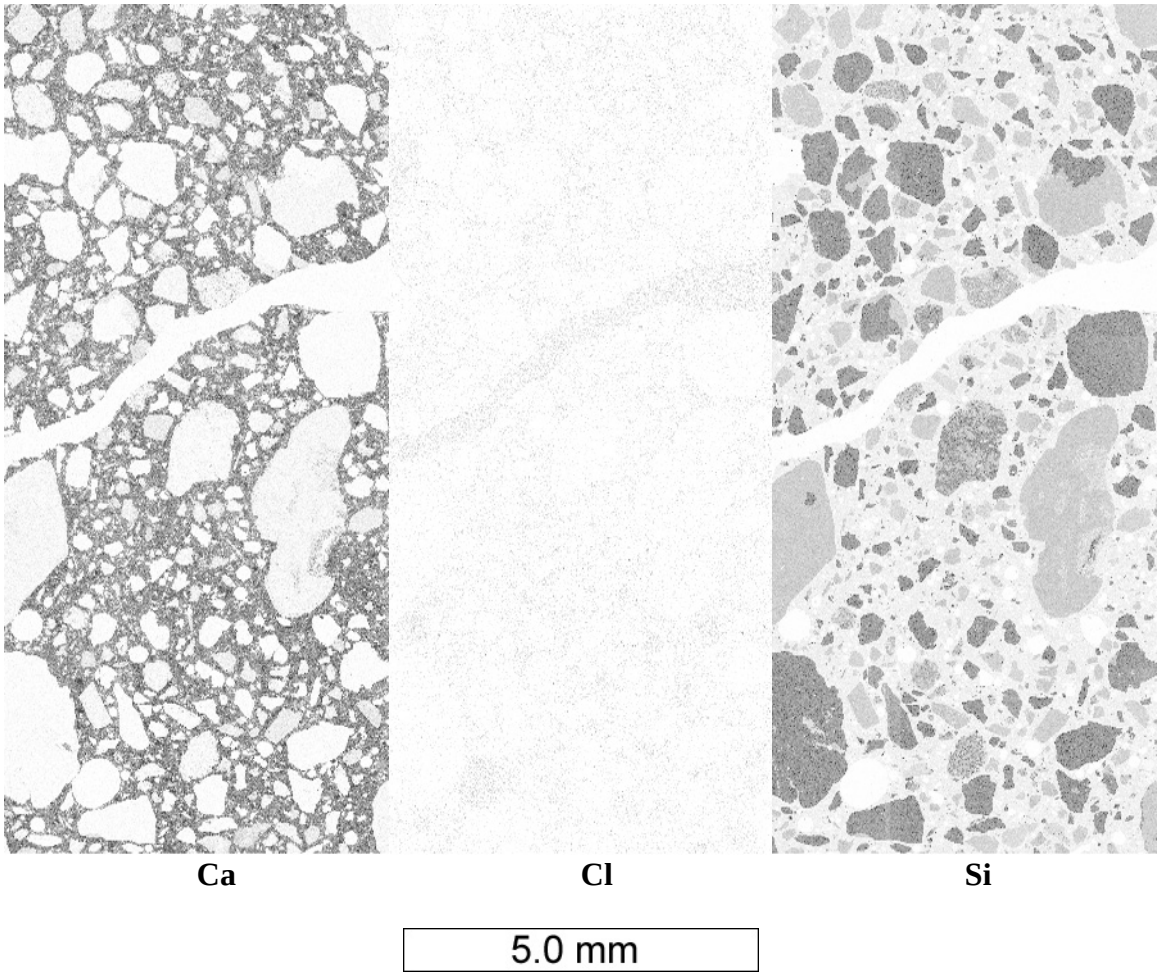

Figure 17: Characteristic Kα x-ray maps showing concentrations for calcium, chlorine, and silicon from polished thin section prepared from core T-1 showing cross section through large crack at 4 cm depth. Darker regions correspond to higher x-ray counts.

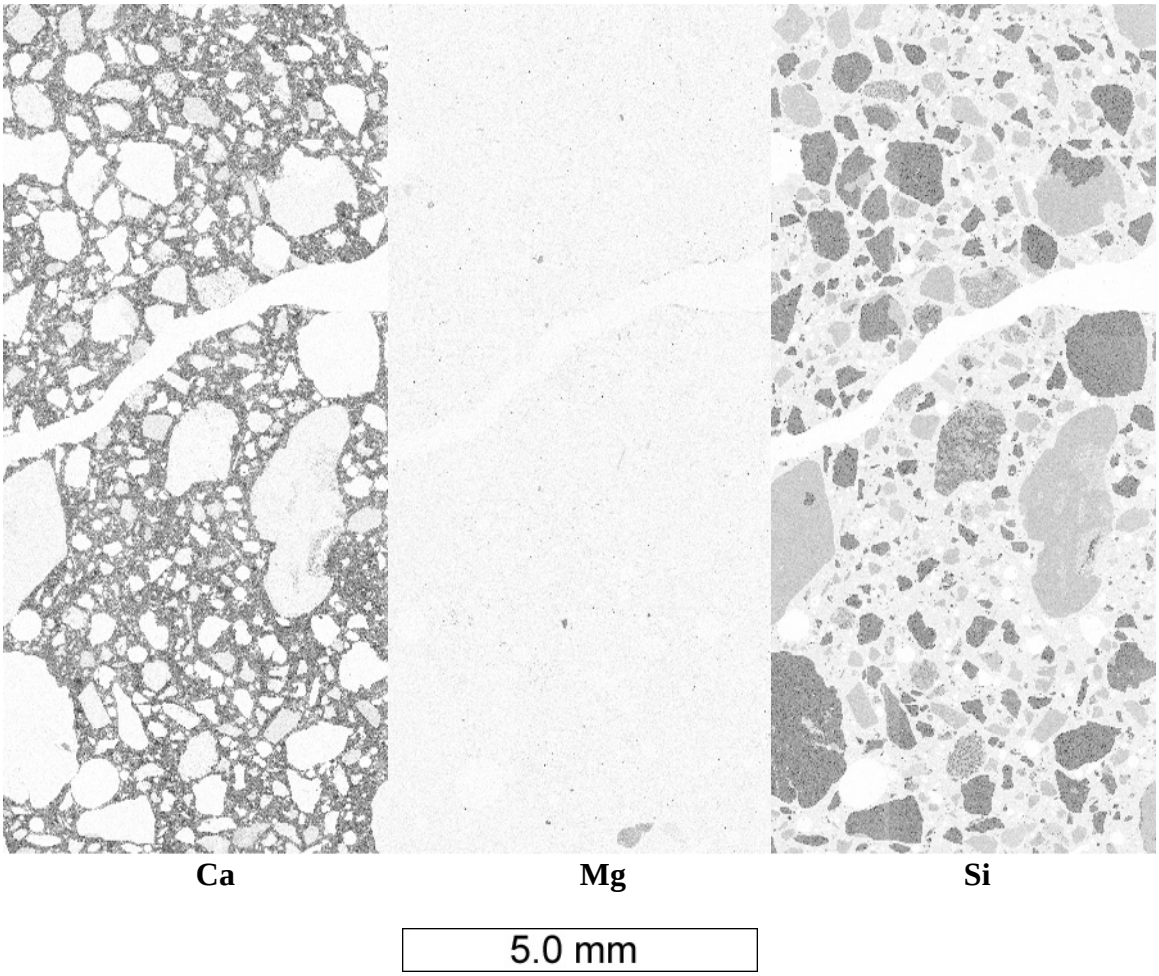

Figure 18: Characteristic Kα x-ray maps showing concentrations for calcium, magnesium, and silicon from polished thin section prepared from core T-1 showing cross section through large crack at 4 cm depth. Darker regions correspond to higher x-ray counts.

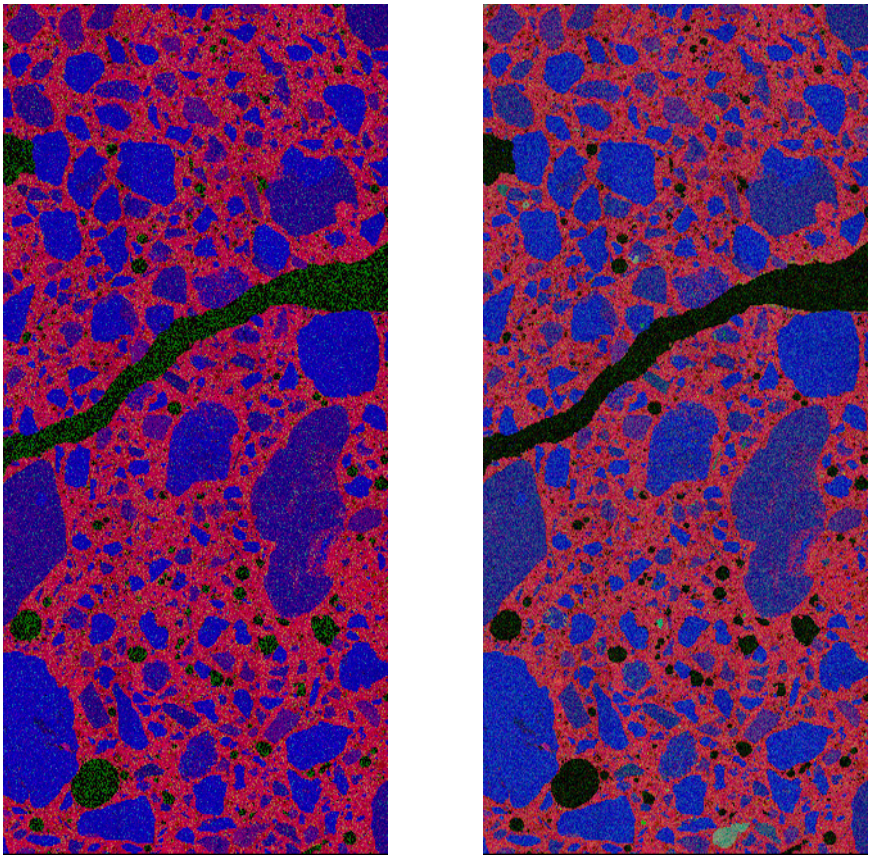

Figure 19: RGB composite image of characteristic Kα x-ray maps from polished thin section prepared from core T-1 showing cross section through large crack at 4 cm depth. Brighter regions correspond to higher x-ray counts.

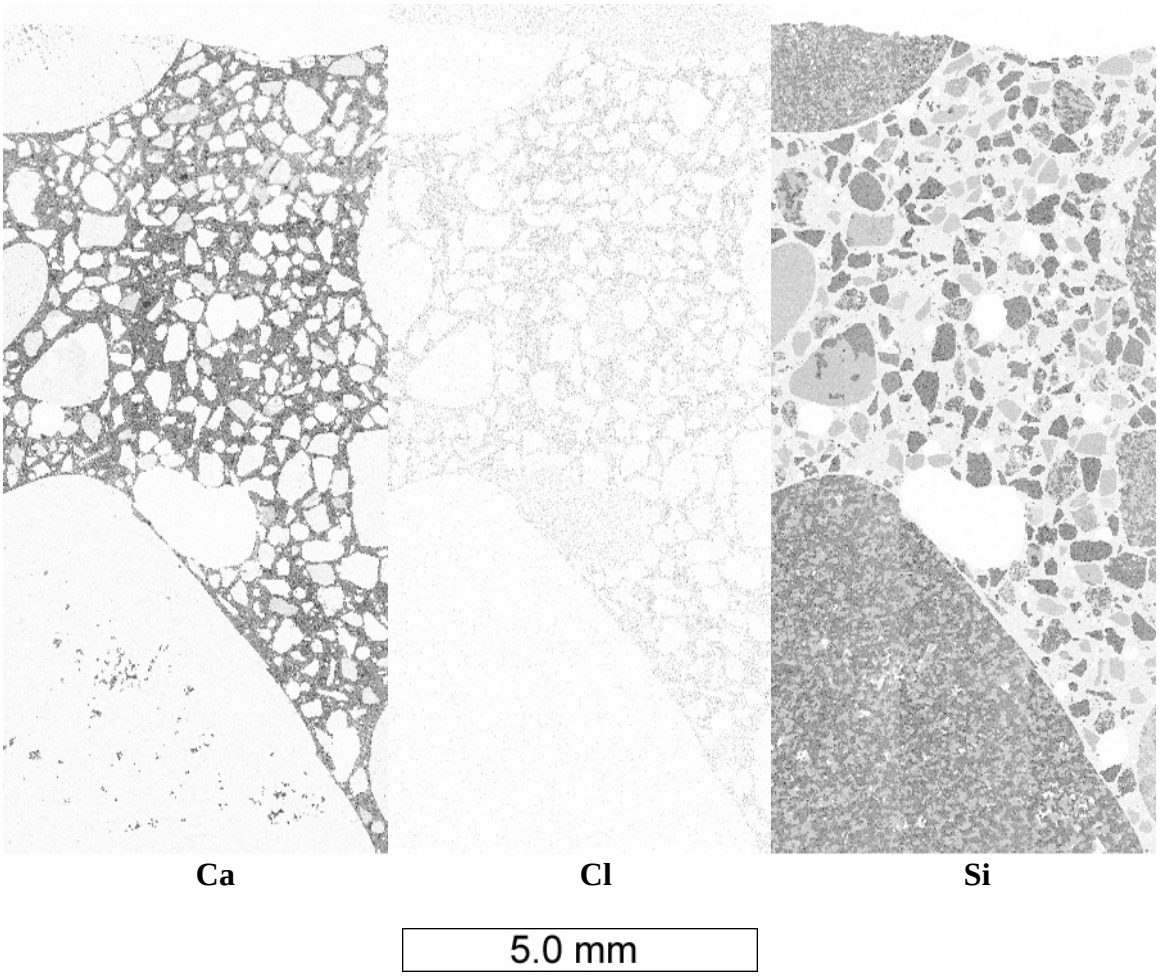

Figure 20: Characteristic Kα x-ray maps showing concentrations for calcium, chlorine, and silicon from polished thin section prepared from core S-1 showing cross section through pavement surface. Darker regions correspond to higher x-ray counts.

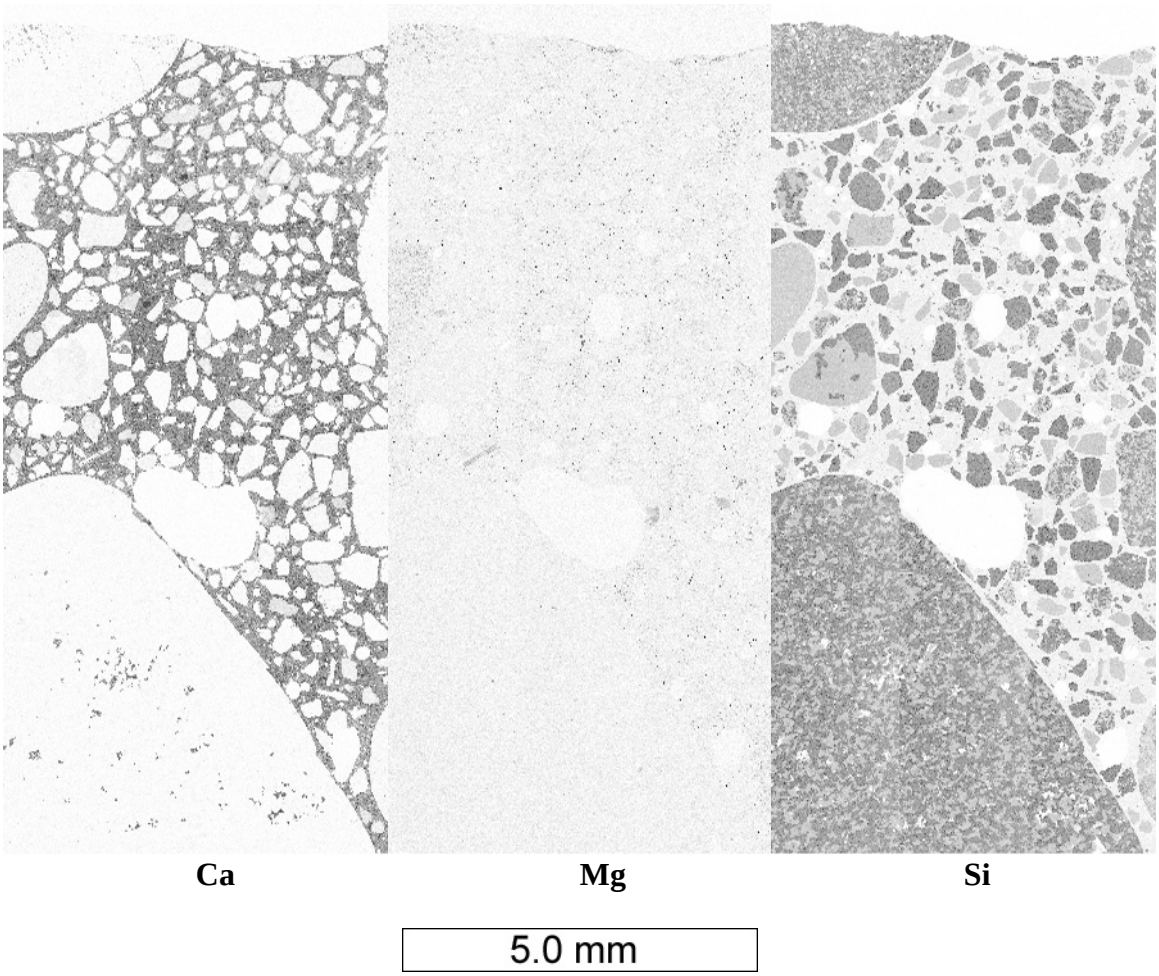

Figure 21: Characteristic Kα x-ray maps showing concentrations for calcium, magnesium, and silicon from polished thin section prepared from core S-1 showing cross section through pavement surface. Darker regions correspond to higher x-ray counts.

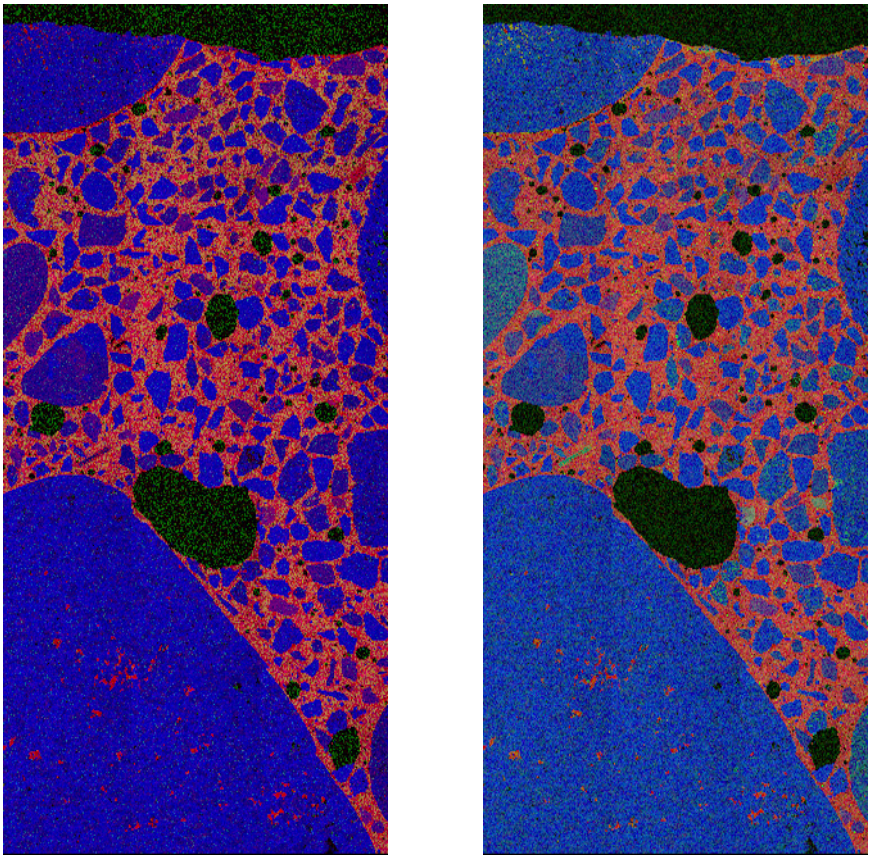

Figure 22: RGB composite image of characteristic Kα x-ray maps from polished thin section prepared from core S-1 showing cross section through pavement surface. Brighter regions correspond to higher x-ray counts.

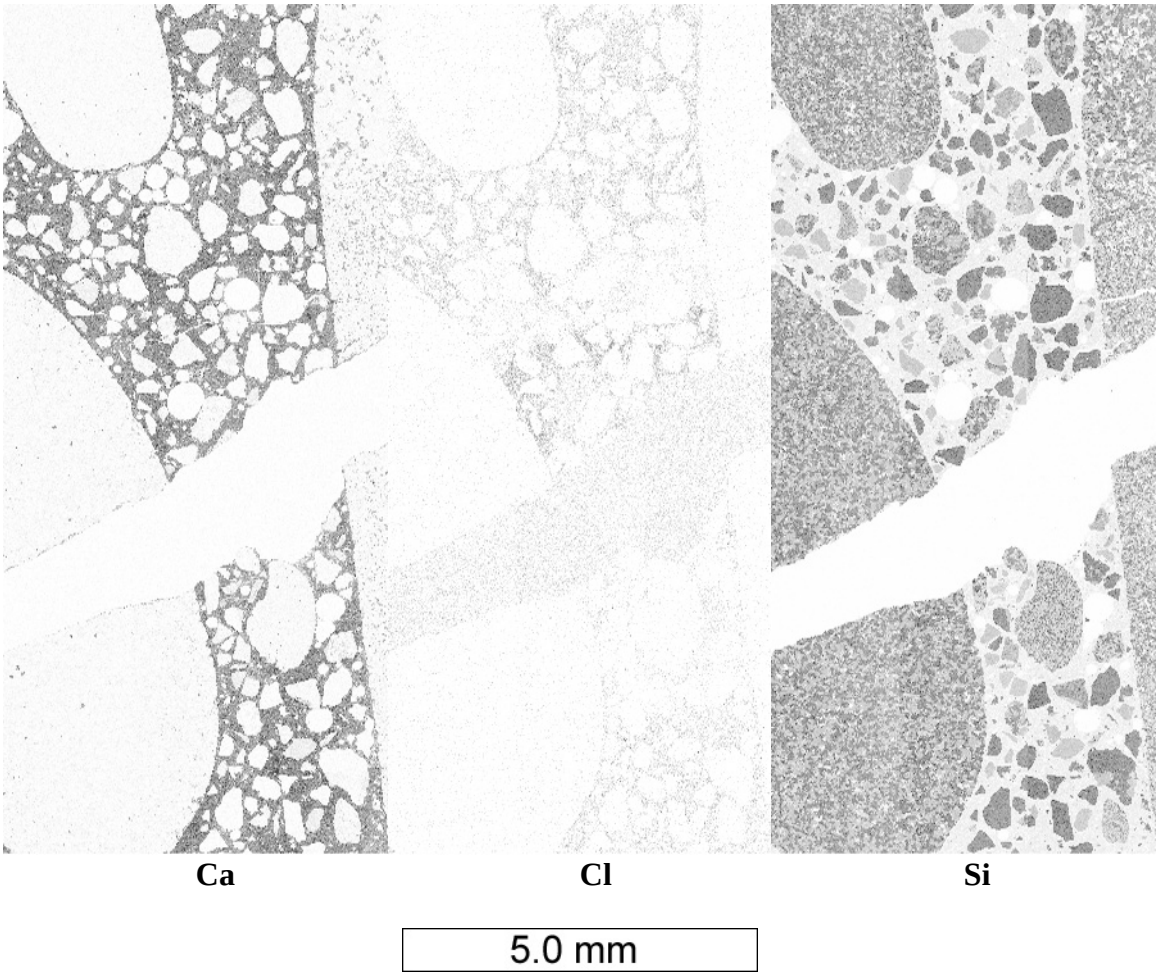

Figure 23: Characteristic Kα x-ray maps showing concentrations for calcium, chlorine, and silicon from polished thin section prepared from core S-1 showing cross section through large crack at 4 cm depth. Darker regions correspond to higher x-ray counts.

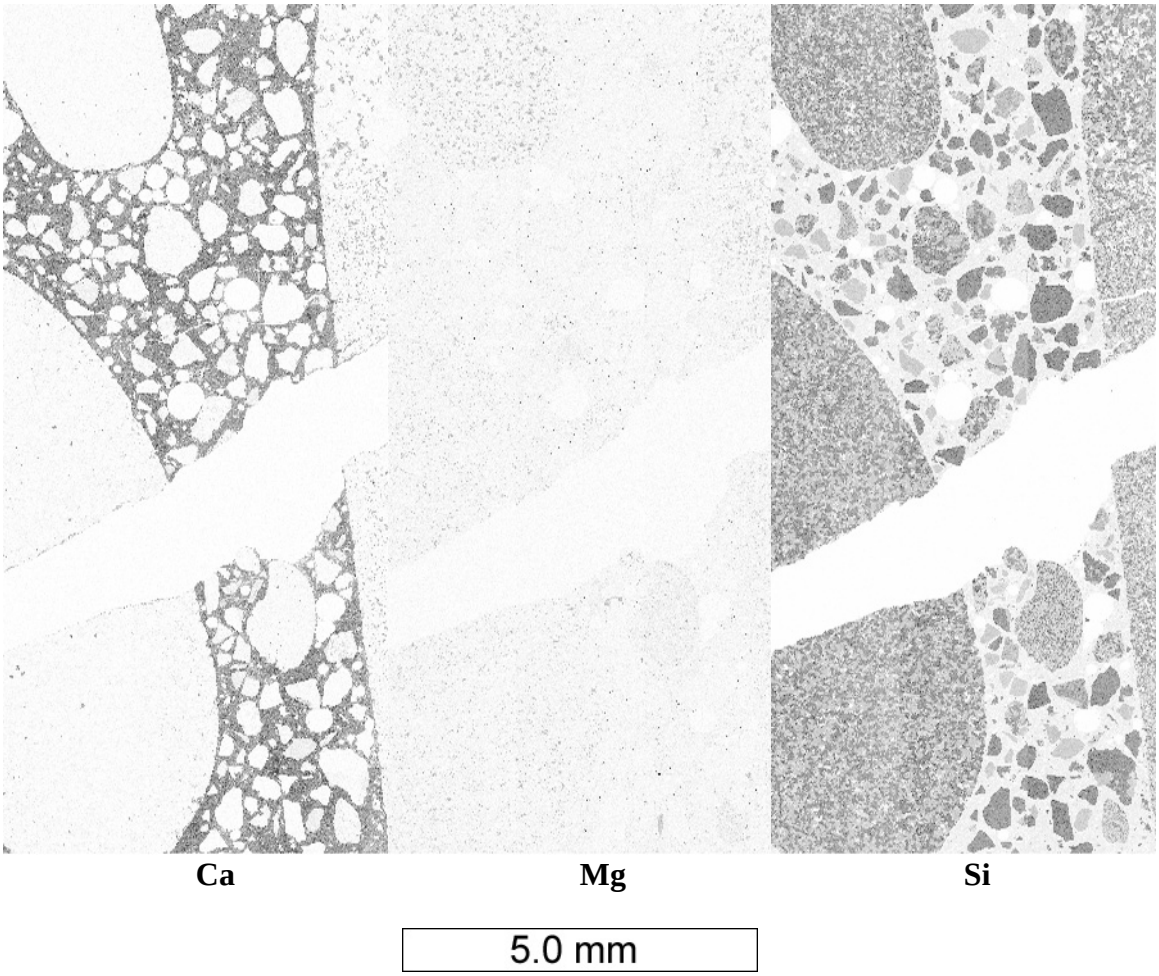

Figure 24: Characteristic Kα x-ray maps showing concentrations for calcium, magnesium, and silicon from polished thin section prepared from core S-1 showing cross section through large crack at 4 cm depth. Darker regions correspond to higher x-ray counts.

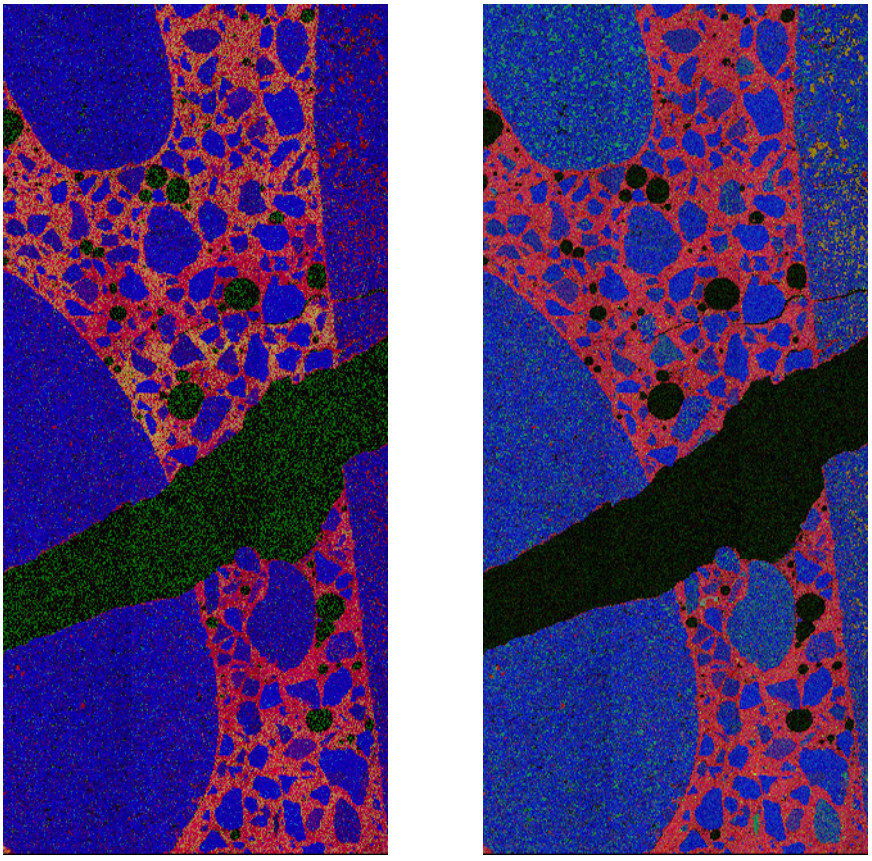

Figure 25: RGB composite image of characteristic Kα x-ray maps from polished thin section prepared from core S-1 showing cross section through large crack at 4 cm depth. Brighter regions correspond to higher x-ray counts.

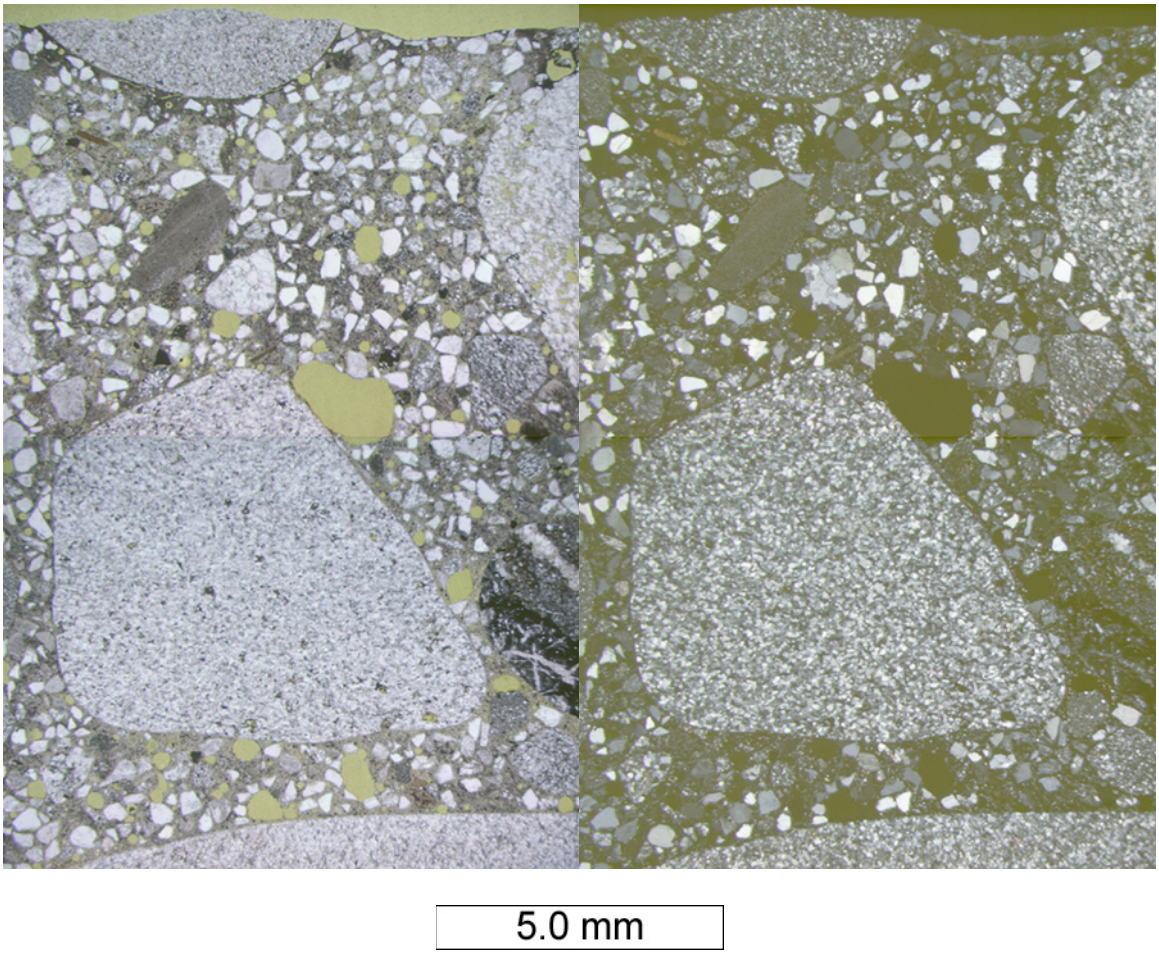

Figure 26a: Plane polarized, (left) and cross polarized, (right) images from polished thin section prepared from core S-1 showing cross section through pavement surface.

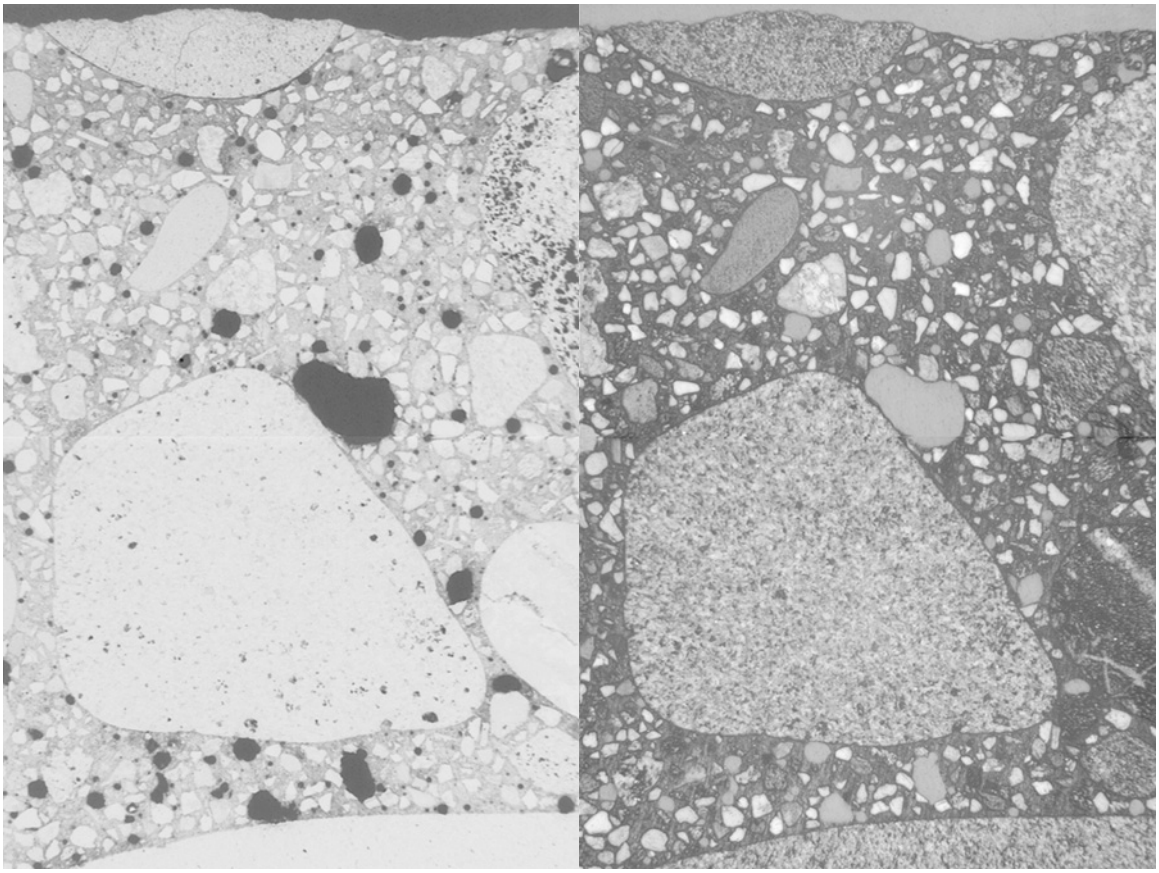

Figure 26a: Epifluorescent, (left) and reflected light, (right) images from polished thin section prepared from core S-1 showing cross section through pavement surface. The epifluorescent image is inverted, so that porous regions appear darker, and denser regions appear lighter.

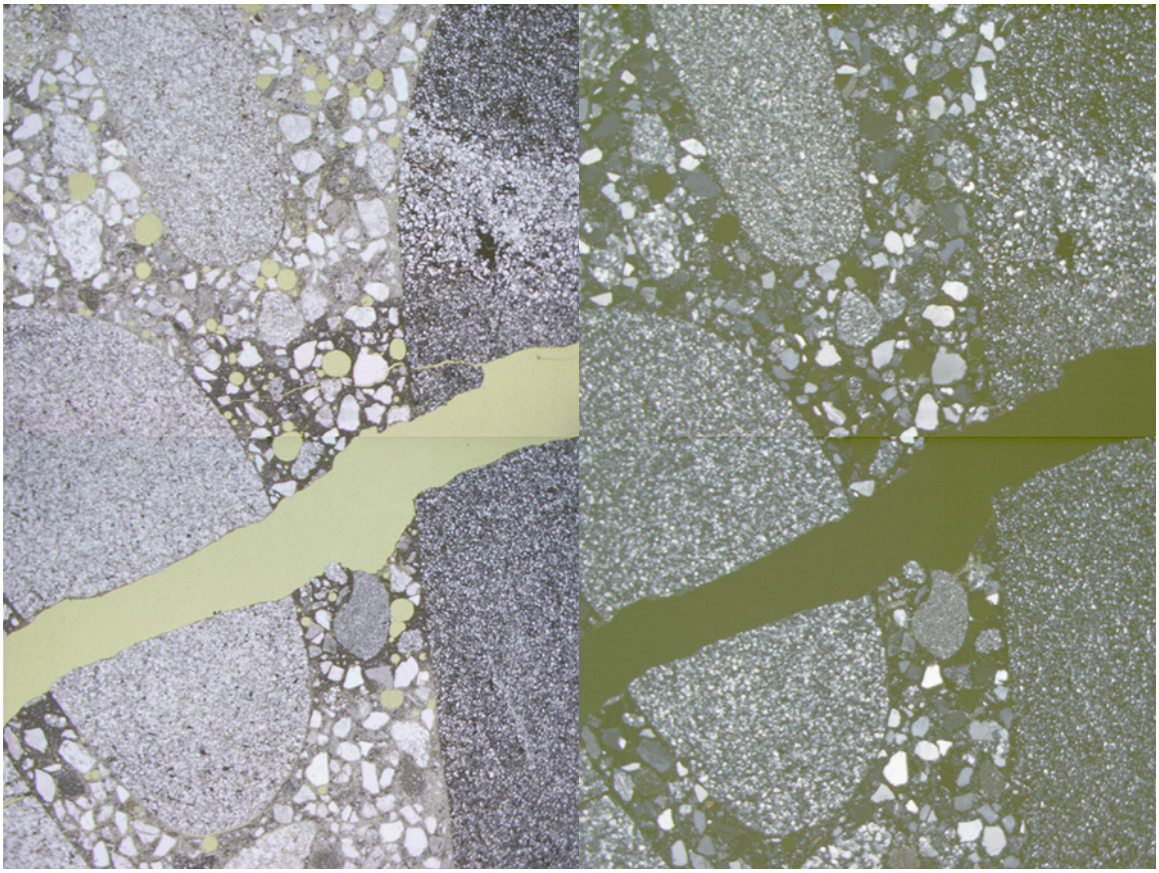

Figure 26a: Plane polarized, (left) and cross polarized, (right) images from polished thin section prepared from core S-1 showing cross section through large crack at 4 cm depth.

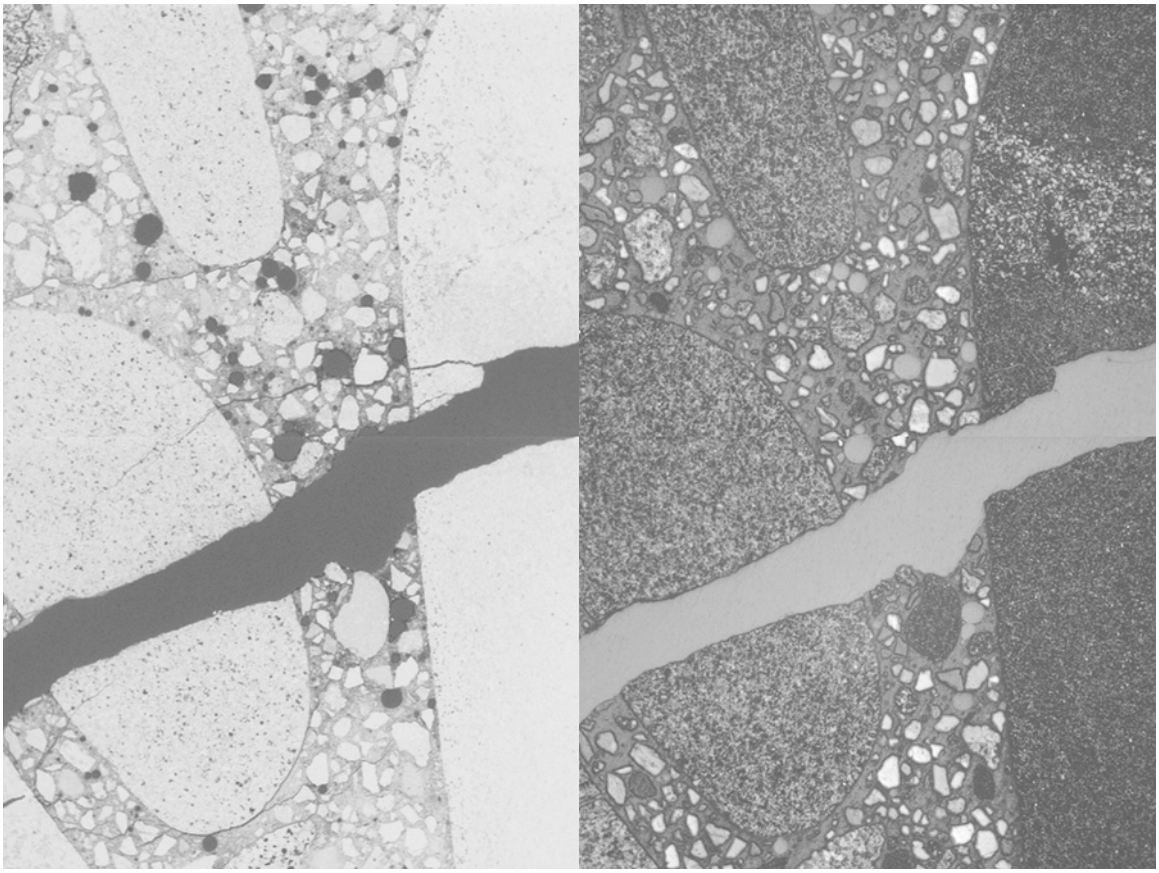

Figure 26a: Epifluorescent, (left) and reflected light, (right) images from polished thin section prepared from core S-1showing cross section through large crack at 4 cm depth. The epifluorescent image is inverted, so that porous regions appear darker, and denser regions appear lighter.

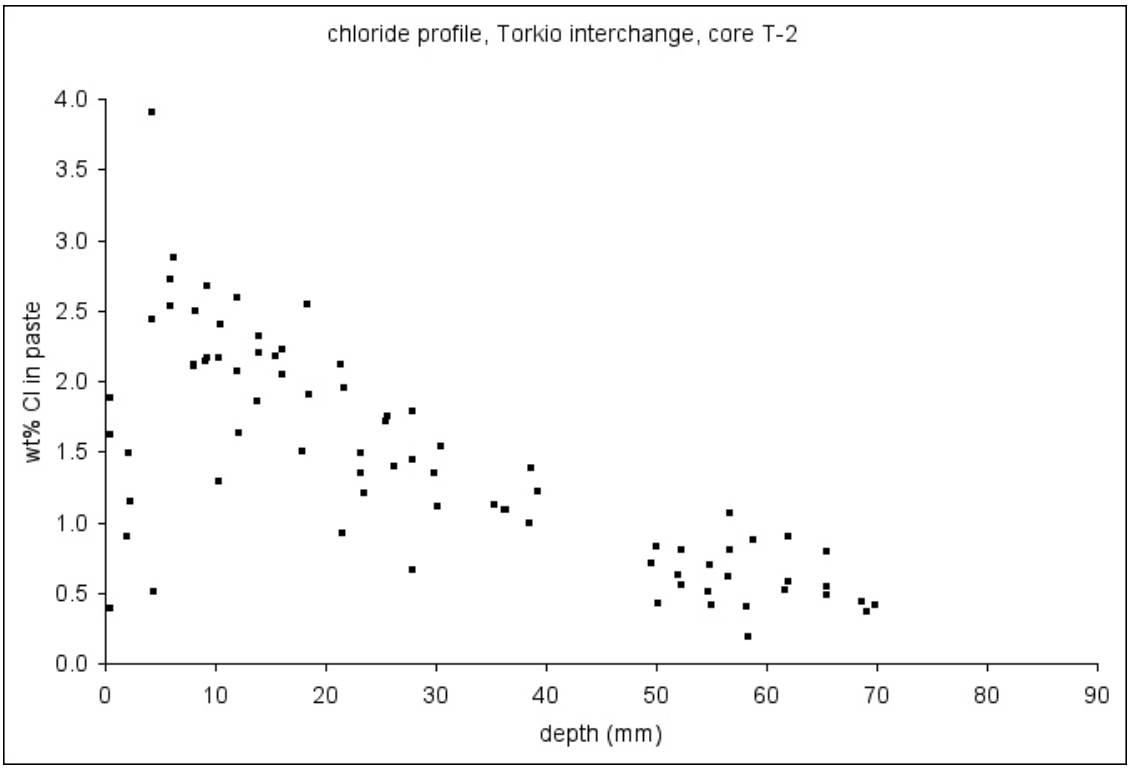

Figure 28: First chloride profile from core T-2

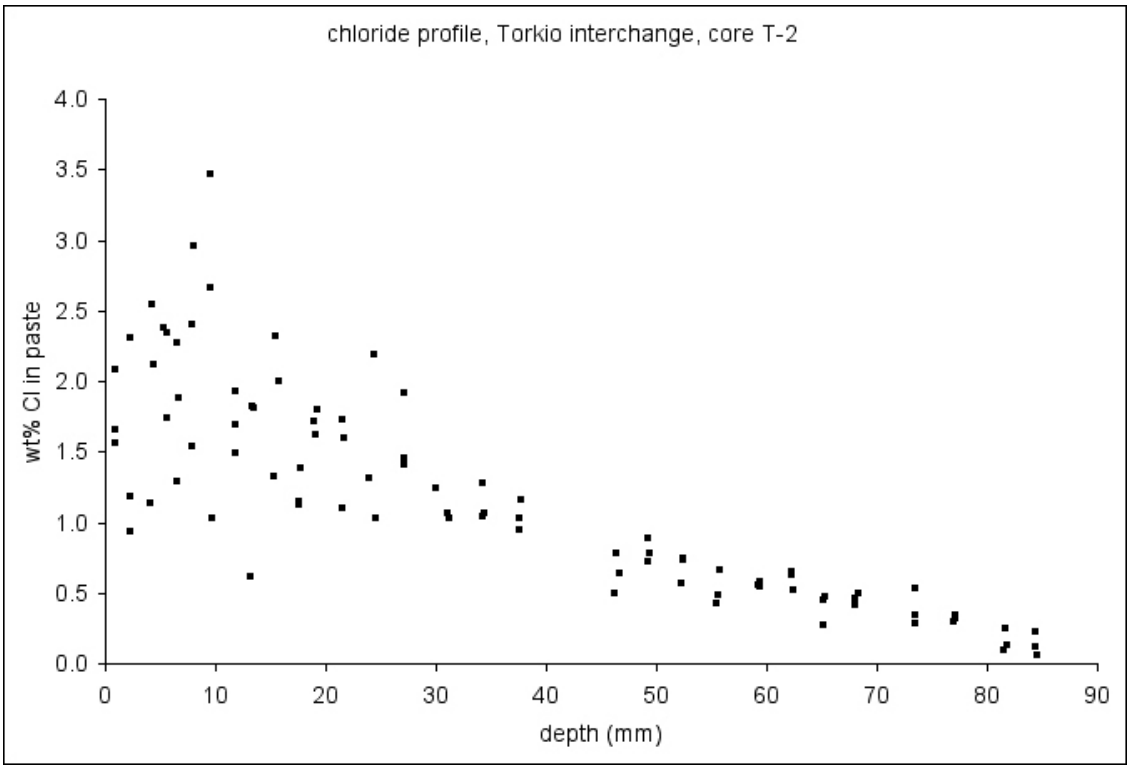

Figure 29: Second chloride profile from core T-2.

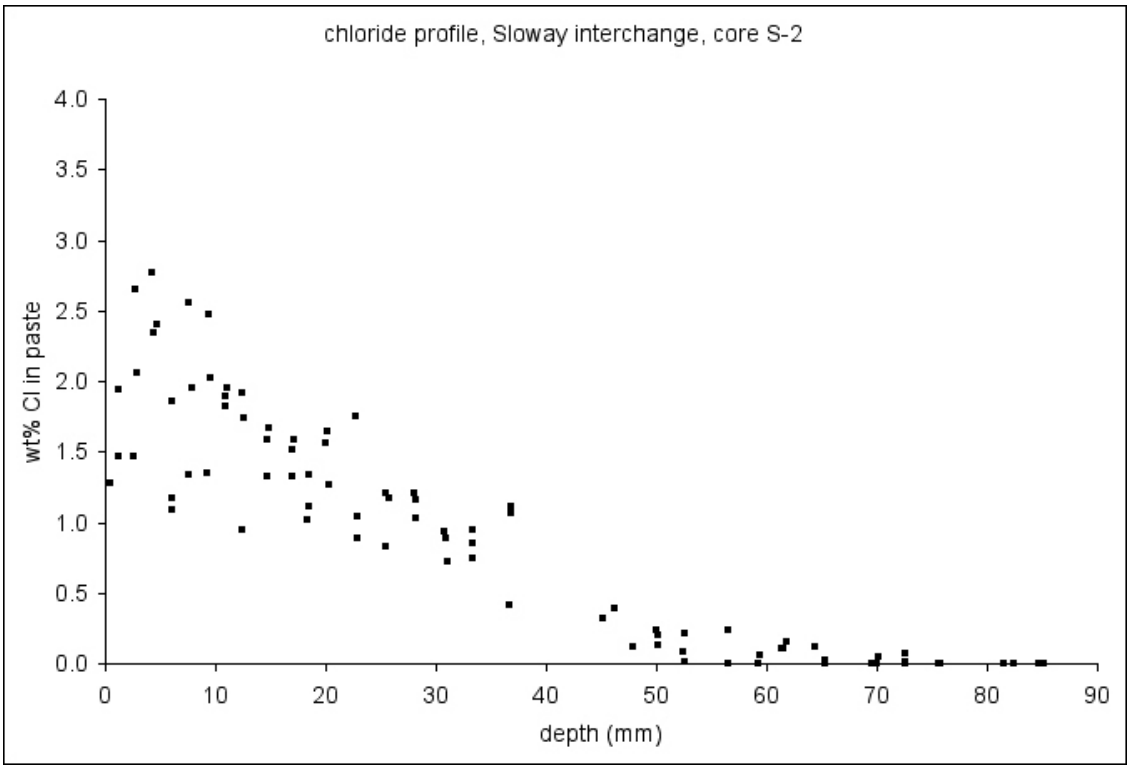

Figure 30: First chloride profile from core S-2.

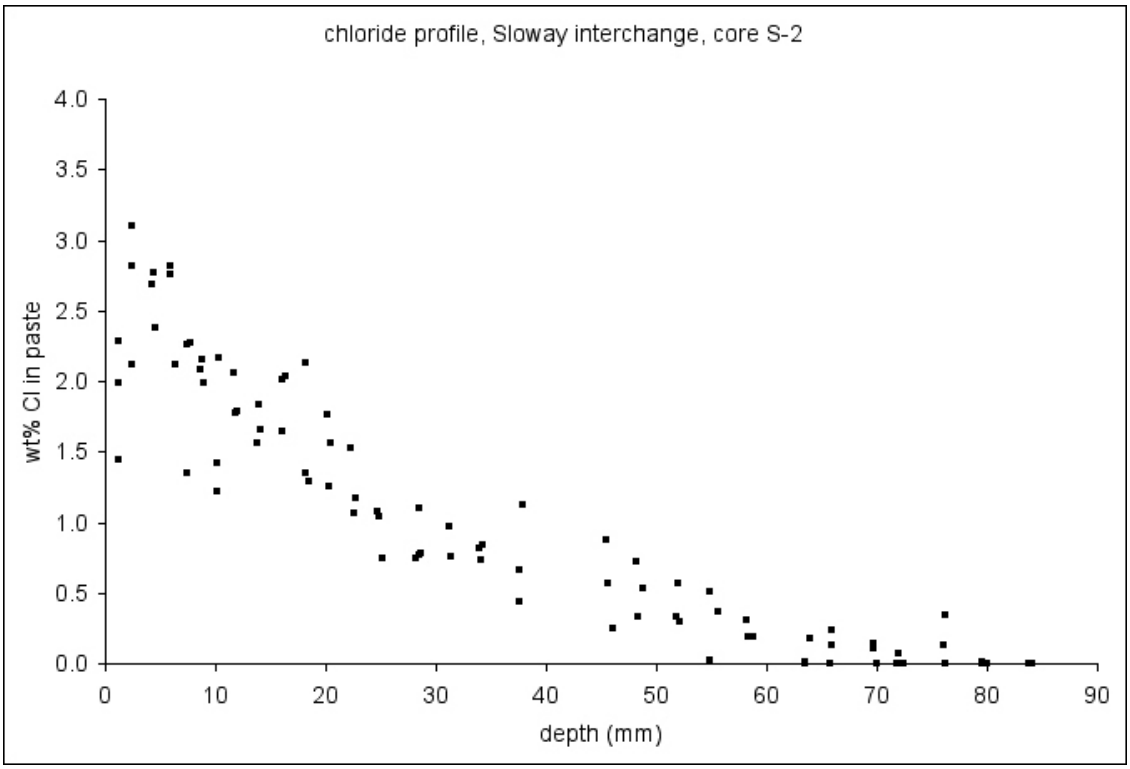

Figure 29: Second chloride profile from core S-2.

Lime solution

NaCl solution

$CaCl_2$ solution

$MgCl_2$ solution

CMA solution

Figure 30: Prisms representative of the five different solutions after 56 days of ASTM C 672 testing.

Task 6: Laboratory Experiment

Work on Phase II of the laboratory experiments has continued. However, based upon preliminary results, it has been determined that the current approach being used in Phase II may not lead to useful data for determining the effects of the various deicers on concrete. Current Phase II testing includes performing the scaling test defined by ASTM C 672. This test deviates from the standard ASTM C 672 test by using solution strengths equal to those used in Phase I for all deicing chemicals tested. The high concentration solutions being used result in solutions that don't freeze. Hence, minimum scaling has been observed with the worse being observed for the control samples ponded with lime water. The ASTM C 672 testing was halted at 56 days and samples have been selected for petrographic examination and chloride profiling. Selected samples are presented in Figure 30 above. Besides modest scaling, sub-parallel cracking was observed on the perimeter of the $CaCl_2$ specimens. This deterioration will be examined petrographicly.

Figure 31: Cracks parallel to ponding surface along sides of prisms just below the pink edge dams typical of prisms exposed to $CaCl_2$ solution, and not observed on prisms exposed to other solutions.

A new approach for Phase II has been developed and is presented below. The new approach will center on the cold temperature immersion test conducted in Phase I but will be conducted with concrete specimens. Additionally, selected mortar specimens will be tested to confirm the results of Phase I and obtain fundamental material properties of the

mixtures tested (e.g. sorptivity, chloride ion penetration, diffusivity). It should be noted that ASTM C 672 testing will be continued at the University of Toronto including determination of the pessimum solution strength of magnesium chloride to cause scaling. The new Phase II experimental plan is presented below.

Revised Phase II Experimental Plan – October 2005

The modified Phase II experimental plan will continue to investigate the effect the various deicers have on concrete. Based on the results to-date, it has been determined that the best approach is to expand the use of the cold temperature testing (@ 40^{o} F), repeating some aspects of the mortar experiment as well as evaluating the impact on concrete . In addition, sorptivity and permeability testing will also be conducted.

The control concrete mixture used in this testing will made with a high quality, partially crushed gravel coarse aggregate (maximum aggregate size of 1 in), natural sand, 564 lb/yd^3 type I cement, a vinsol resin air entraining agent (air content of 6 ± 1 percent), and a water-to-cementitious materials ratio (*w/cm*) of 0.42. The slump will be 3 ± 0.5 in. Additionally, a 0.55 *w/cm* will also be tested, as will mixtures made with a class F fly ash (15% replacement by weight) and ground blast furnace slag (30% replacement by weight). A constant paste volume will be maintained for all mixtures. The purpose of using two values of *w/cm* is that with a low *w/cm*, as shown in Phase I, the observed deterioration moves at a slower rate. Given that the rate of deterioration is unknown, a higher *w/cm* may allow for observation of deterioration that might be only partially or slightly apparent with a lower value of *w/cm.* Also, the higher *w/cm* will represent what is occurring in lower grade concrete or concrete that has been placed after water addition at the job site.

Table 1 presents the experimental design for this phase of the experiment. The top two rows present the various mixtures that will be tested. The third row indicates the sealants to be tested, with the "U" meaning unsealed and "S1" and "S2" meaning sealants 1 and 2 (these being commercially available silanes/siloxane sealants). The left most column indicates the deicer to be used and concentration (low or high as shown in Table 2).

The specimens will be cylindrical, 4 inch diameter specimens, nominally 2 inches in height and will be submerged in deicer solutions at the concentrations listed in table 2. Each week, the solution will be replaced, with the specimens removed from solution after 56 and 84 days of submersion for analysis of deicer penetration and degradation.

Table 1. Experimental design for Phase II testing.

Mixture Type		**Portland Cement**						**Class F Fly Ash**						**GBFS**					
w/cm		**0.42**			**0.55**			**0.42**			**0.55**			**0.42**			**0.55**		
Sealant		**U**	**S1**	**S2**	**U**	**S1**	**S2**	**U**	**S1**	**S2**	**U**	**S1**	**S2**	**U**	**S1**	**S2**	**U**	**S1**	**S2**
Deicer																			
None		2			2			2			2			2			2		
NaCl	L	2			2														
	H	2			2														
$CaCl_2$	L	2			2	2	2				2	2	2				2	2	2
	H	2			2	2	2	2			2	2	2	2			2	2	2
$MgCl_2$	L	2			2	2	2				2	2	2				2	2	2
	H	2			2	2	2	2			2	2	2	2			2	2	2
CMA	L	2			2														
	H	2			2						2						2		
Proprietary	L	2			2														
	H	2			2						2						2		
Total		22			22	8	8	6			14	8	8	6			14	8	8

Table 2. Deicer concentrations to be used in the Phase II testing.

Deicer	**Concentration (%)**	
	Low	**High**
NaCl	8.9	17.8
$CaCl_2$	8.5	17.0
$MgCl_2$	7.5	15.0
CMA	12.5	25.0
Proprietary	TBD	TBD

In addition to the concrete testing, certain elements of the mortar testing will be repeated and expanded. This work will focus exclusively on specimens submerged in $CaCl_2$, $MgCl_2$, and the proprietary deicer. Cylindrical mortar specimens will be made with Portland cement, fly ash, and GBFS blends at *w/cm* ratios of 0.42 and 0.55 and submerged in deicer solutions at the same concentrations listed in table 2. Each week, the solution will be replaced, with the specimens being analyzed after 56 and 84 days of submersion. The experimental plan is summarized in Table 3.

Table 3. Experimental design for cylindrical specimens tested at 40 ^{o}F.

Mixture Type		**Portland Cement**		**Fly Ash**		**GBFS**	
w/cm		**0.42**	**0.55**	**0.42**	**0.55**	**0.42**	**0.55**
Deicer							
None		4	4	4	4	4	4
$CaCl_2$	L		4		4		4
	H	4	4	4	4	4	4
$MgCl_2$	L		4		4		4
	H	4	4	4	4	4	4
Proprietary	L		4		4		4
	H	4	4	4	4	4	4
Total		16	28	16	28	16	28

Diffusion and Permeability Assessment

Additional cylindrical concrete specimens will be cast for diffusion and permeability testing. Two specimens for each deicer/concentration combination will be prepared and submerged in solution at 40 ^{o}F for to determine the diffusion coefficient. Rapid chloride permeability testing (in accordance with ASTM C 1202) and sorptivity testing will also be conducted to provide an assessment of permeability.

Task 6 Problems and/or Deviations from Work Plan

There were no problems for Task 6 incurred during the reporting period. However, based upon preliminary results, the Task 6 approach is being modified as described above.

Task 6 Completion -60%

Task 8: Effects of Various Deicing Chemicals

No additional work has been conducted on Task 8. Further work will continue once specimens from the Phase II experiments are ready for analysis.

Task 8 Completion -25%

Task 11 Submit Interim Report

Task 11 Completion - 100%

Task 12 Meeting with Technical Panel at Michigan Tech

Task 12 Completion - 100%